Self-Assembly at the Prebiotic Solid−Liquid Interface: Structures of Self-Assembled Monolayers of Adenine and Guanine Bases Formed on Inorganic Surfaces

Stephen J. Sowerby,† Michael Edelwirth, and Wolfgang M. Heckl*

Ludwig Maximilians Universität München, Institüt für Kristallographie, Theresienstr. 41, 80333 München, Germany

Received: January 6, 1998; In Final Form: April 20, 1998

Previously proposed models of monolayers of adenine and guanine, based on scanning tunneling microscopy and atomic force microscopy images, have been critically examined. We have applied molecular mechanics computer simulations to these models and, where appropriate, examined additional scanning tunneling microscopy data. These findings support the proposed adenine structure based on low-energy diffraction analysis and molecular mechanics but indicate that the structure of the guanine monolayer on graphite is different from those previously proposed. These findings indicate that the energy-minimized adsorbate stuctures of both adenine and guanine form a similar molecular configuration on both graphite and molybdenum disulfide surfaces. It is speculated that the formation of these structures may have had some prebiotic relevance.

Introduction

The formation of monolayers of the purine and pyrimidine bases through physisorption-mediated molecular self-assembly at the solid−liquid interface has been proposed to have a functional role in the emergence of terrestrial life.[1,2] Inherent in these proposals was the prebiotic availability of the nucleic acid purine and pyrimidine derivatives for which there are arguments both for[3] and against.[4] Despite contradictory discussion, the central role of these molecules in the modern biochemical machinery dictated their appearance at some early stage during chemical evolution and justifies their examination in a prebiotic context. Models for the emergence of life that implicate the ordering of monomers on the surfaces of crystals have been established for some time[5,6] and have recently invoked the crystalline surfaces of metal sulfides.[1,2,7−9]

The application of near-field microscopy techniques, namely, scanning tunneling microscopy (STM)[10] and atomic force microscopy (AFM),[11] to surface structures has allowed real space analysis with atomic scale lateral resolution. STM and electrochemical applications of this (ECSTM) have been applied to study the inorganic crystal surfaces of graphite {0001}[12] and metal sulfides, including the surface of molybdenite (MoS_2) {0001},[13,14] iron pyrite (FeS_2) {100},[15,16] {101},[15,17] ruthenium pyrite (RuS_2) {100},[18] and galena (PbS_2) {100},[15,19] {001}.[20−24] These studies suggest that STM examination of prebiotically relevant minerals and their interactions with organic compounds may provide some evidence for processes that lead to the emergence of life.

Literature detailing studies of two-dimensional adsorbate structures of the nucleic acid bases at the mercury−water interface has been reviewed,[25] as has their self-assembly at the solid−liquid interface.[2,26] The examination of self-assembled organic thin films has been justified with applications in separation science,[27] optoelectronics,[28] corrosion inhibition,[29] and supramolecular chemistry.[30] It has been suggested that purine and pyrimidine monolayers could be candidates for a stationary phase in organic molecule separation systems and as templates for the assembly of higher ordered polymers at the prebiotic solid−liquid interface.[1,2] These structures may also have practical applications.[31,32]

Inherent in the understanding of these systems is a detailed and precise knowledge of the monolayer structure. The application of STM and AFM has proved particularly well suited to the study of the molecular arrangement of close-packed adsorbate structures on the surfaces of inert layered compounds such as graphite and MoS_2. Relevant examples include cyclic aromatic compounds,[33] long-chain alkane derivatives,[34] and cyanobiphenyl liquid crystal derivatives.[35] Structural models for monolayers of purine and pyrimidine derivatives based on adsorbate STM images obtained on graphite,[1,36−48] and MoS_2 surfaces[1,32,38,39,41] have been presented. Similar studies have been performed on reconstructed gold[49,50] and copper surfaces.[51−53] Some of these systems have also been complemented by low-energy electron diffraction (LEED) studies[54] and molecular mechanics (MM) simulations.[2,32,54−56]

Model building based on the interpretation of the experimental STM data has, however, been somewhat variant and has been subject to a process of refinement as an understanding of the physical principles directing monolayer formation has developed. Indeed, the interpretation of the complex STM image contrast mechanism for these and other organic systems is not straightforward and in some cases employs a quantum chemical approach.[57−60] The complementary use of both graphite and MoS_2 surfaces in STM experiments of monolayer structure determination has aided the interpretation because of the substrate-dependent differences in the STM image contrast of the adsorbates.[1,38,39,41,56]

It is the purpose of this communication to critically evaluate the previously proposed packing structures of the purine base monolayer systems by the application of MM. It is also intended to indicate how examination of these organic monolayer structures by STM/AFM, together with MM simulations and other available data, can lead to a reasonable structure deter-

* To whom correspondence should be addressed. Telephone: +49 89 2396 4331. Fax: +49 89 2396 4331. E-mail: w.heckl@lrz.uni-muenchen.de.
† Permanent address: Department of Biochemistry, University of Otago, P.O. Box 56, Dunedin, New Zealand.

S1089-5647(98)00684-1 CCC: $15.00 © 1998 American Chemical Society
Published on Web 07/07/1998

mination of the monolayer adsorbate. This examination has been restricted to adenine and guanine, for which possible prebiotic syntheses have been described.[3] It is hoped that the refined analysis of these pure systems will provide a solid base for further theoretical and experimental examinations of potentially prebiotic processes at the solid−liquid interface.

Methods

Computer simulation of chemical systems through MM provides a practical treatment of atomic and molecular structures that are not particularly demanding in terms of computational power or time. MM treats these systems as physical models and applies empirically measured properties in terms of the potential energy hypersurface (PES). MM was applied to models of the purine and pyrimidine monolayers physisorbed on the surfaces of graphite and MoS_2 surfaces with the program Cerius[2] running on a Silicon Graphics Indigo II workstation. For the energy minimization calculations, we used the Dreiding II force field,[61] which has been parametrized for organic, biological, and main group inorganic molecules and has an explicit hydrogen-bonding term. The potential energy (E_T) of a chemical system is the sum of the two-, three-, and four-body terms in the energy expression that is implemented by Cerius:[2]

$$E_T = E_{bond} + E_{angle} + E_{torsion} + E_{inversion} + E_{vdW} + E_{Coulombic} + E_H$$

The valence terms E_{bond} (bond stretching), E_{angle} (angular distortions), $E_{torsion}$ (dihedral angle torsions), and $E_{inversion}$ (umbrella inversions) relate to specific bond and atomic orientations of the molecular structure and were modeled by classical mechanics expressions fitted to reproduce spectroscopic and crystallographic data. The nonbond terms E_{vdW} (van der Waals), $E_{Coulombic}$ (electrostatic), and E_H (hydrogen bonding) relate to intermolecular interactions. The van der Waals term was modeled using a Lennard-Jones 12-6 potential, whereas the hydrogen bond applies the Lennard-Jones 12-10 potential and includes an angle-dependent $\cos\theta$ term. Electrostatic interactions took the form of a Coulombic point charge interaction between atom-centered partial charges. Long-range electrostatic and van der Waals interactions were treated with the Ewald summation technique.

Both graphite and the natural polymorphic form of crystalline MoS_2 (2*H*-MoS_2) used in STM experiments consist of a lamella structure composed of covalently bonded layers held together by weak (van der Waals) interlayer interactions. Upon cleavage of their (0001) planes, they do not undergo physical reconstruction at the surface. Calculation of the interlamella specific surface energy of MoS_2 showed a value comparable to that of graphite and that was in close agreement with experimental results.[62] Although the surface structures of these cleaved materials may be deformable by STM in air, for the purposes of computer simulation of the monolayer structures, they were treated as rigid and not subject to energy minimization.

The two-dimensional monolayer systems were modeled as a molecular solid of infinite dimensions using periodic boundary conditions in a three-dimensional crystal model space of *P*1 symmetry as previously described.[55,56,63,64] The three Cartesian vectors *a*, *b*, and *c* corresponded to the two coincident lattice vectors and the third dimension, respectively.

Determination of the total adsorbate−substrate interaction between an adenine molecule and the graphite surface had been calculated previously by including in the energy expression an electrostatic term related to the polarizability of the carbon in the graphite surface. This was determined to be negligible, and the interaction was adequately described by the Lennard-Jones 12-6 potential.[55] The parametrization of the cleaved MoS_2 surface and its complete interaction with adenine molecules will be detailed in a separate communication.[65]

The restriction of the adsorbate molecules to the observed coincident mesh was facilitated by the imposition of periodic boundary conditions to a fixed simulation cell of the coincident mesh dimensions. The measured mesh dimensions were the only empirical parameters that we have placed on the adsorbate−substrate interaction. Although an adsorbate−substrate van der Waals term is approximated through the force field, the electrostatic component is neglected. In the absence of a complete description of the adsorbate−substrate interaction, the periodic boundary conditions simulate the effects of both the adsorbate−adsorbate and the adsorbate−substrate interactions in the two-dimensional plane of the adsorbate and *not* the specific adsorbate−substrate interaction that a lone molecule would experience on the surface. This approach has been previously applied to adenine[32,54] and uracil[56] monolayers formed on graphite and MoS_2 surfaces.

The substrate model surfaces were the {0001} surfaces of graphite and 2*H*-MoS_2 bulk crystal models. Convergence calculations were used to determine the depth of the model bulk solid, which corresponded to a four-layer slab of graphite[55] and a three-layer slab of MoS_2.[32] The length of the cell perpendicular to the surface (*c*) was extended to 15 nm to ensure no artifactual effects of ghost molecules generated by the adjacent cells from the periodic boundary conditions. The model surface mesh dimensions (*a*, *b*) were that of the adsorbate coincident mesh determined by comparison of the real space STM images of the adsorbate and of the underlying substrate as presented by the authors of the examined structures. Consequently, only the models invoking coincident mesh dimensions could be tested.

Electrostatic potential derived (ESPD) partial atomic charges and the starting geometry of the atoms of adsorbate molecules and their corresponding dipole moments were calculated by the semiempirical MNDO (modified neglect of differential overlap) augmented AM-1 (Austin method) using the public domain software "MOPAC", accessible through Cerius.[2] Comparison of the semiempirical derived bond lengths and angles with values obtained by ab initio MP2 (second-order Møller−Plesset perturbation theory) level calculations[66] shows good agreement.

For the energy minimization calculations, the model adsorbate molecules were placed manually on the model surface according to the proposed models and subjected to the minimization algorithm. The calculations were terminated when the total energy of the potential energy hypersurface (PES) reached an rms force gradient of 0.03 kcal mol^{-1} $Å^{-1}$. The lattice energy calculations were performed using the theory of the atom−atom potential method for molecular crystals[67] implemented through the Crystal Packer module in Cerius.[2] The determination of the lattice energy of a single molecular species (ΔE_T) was determined by calculating the difference between the model energy (E_T) and the model energy with a single base molecule retracted 5 nm from the surface. These values were determined for adenine on graphite because not all models had equivalent adsorbate composition and the guanine on graphite models were of different lateral dimensions. ΔE_T allows for a direct comparison between different models.

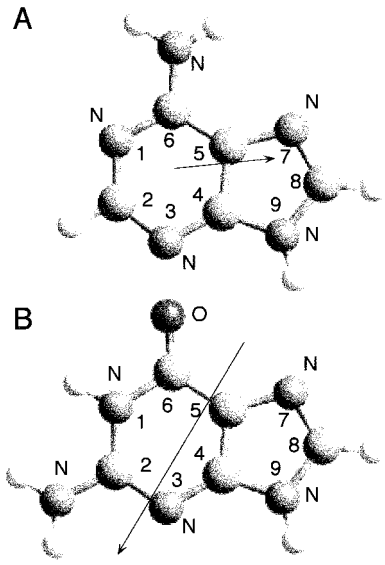

Figure 1. Energy-minimized models of (A) adenine and (B) guanine. The black arrows indicate the magnitude of the dipole moments, which are 2.18 and 5.91 D, respectively.

Results and Discussion

The molecular structure of the purine base, adenine (6-aminopurine, $C_5H_5N_5$), and its intermolecular interactions have been determined by crystallographic studies of the hydrochloride,[68−70] hydrochloride hemihydrate,[71] and dihydrochloride[72] and within mixed component complexes of biological compounds.[73] The literature on the crystal structure of the bulk state of pure adenine does not appear to be readily available. The energy-minimized structure of adenine determined by semiempirical calculation is shown in Figure 1A. The nitrogen bound hydrogens, N(6)H2, and N(9)H and the ring nitrogens N(1), N(3), and N(7) constitute three proton donor and acceptor moieties, respectively.

The molecular structure of the purine base, guanine (2-amino-6-hydroxypurine, $C_5H_5N_5O$), and its intermolecular interactions have been determined by crystallographic studies of the hydrochloride[68] and monohydrate[74] and within mixed component complexes of biological compounds.[73] Similar to adenine, guanine has the ability to undergo amino−imino tautomerism but, additionally, has a keto−enol functionality. As with all of the nucleic acid purines and pyrimidines, only the amino and enol canonical forms have been observed experimentally.[75] The nitrogen bound hydrogens, N(1)H, and N(2)H2, and N(9)H constitute the proton donors. The ring nitrogens, N(3), N(7), and the keto substituent O(6) are the available proton acceptor moieties.

Adenine Monolayers. The structure of adenine monolayers on graphite surfaces has been examined by several authors using a variety of approaches. Allen et al. (1991) demonstrated by STM in air that a lattice of adsorbate molecules formed on the {0001} surface of graphite following evaporation of an aqueous solution at elevated temperature (80 °C). By examining both the adsorbate and then the underlying substrate lattices, they determined the adsorbate epitaxy. Substrate images were not shown. The STM image (and adsorbate packing) was described in terms of bimolecular head-to-tail rows of planar-arranged adenine molecules placed 0.88 ± 0.14 nm apart. Adjacent rows (2.2 nm) were separated by a water channel (1.13 nm), and the adsorbate structure was almost exclusively stabilized by van der Waals type interactions. The adsorbate mesh can be described by the lattice vectors a and b and the angle that separates them, γ ($a = 2.2$ nm, $b = 0.88 \pm 0.14$ nm, $\gamma = 90°$). Molecular dynamics simulation was applied to the proposed model and the presence of water was supported by laser ionization time-of-flight mass spectroscopy, although the data were not shown.[36] These data and interpretation were presented again with the addition of an atomic force microscopy (AFM) image showing only the formation of three-dimensional amorphous structures attributed to the adenine adsorbate.[37] Srinivasan and Murphy (1992) applied ECSTM to adenine adsorption on graphite surfaces in a 0.1 M NaCl electrolyte. The formation of the adsorbate was confirmed by the appearance of a "capacitance pit" on a plot of interfacial capacitance versus electrode potential. The capacitance pit was a function of reduced capacitance following the formation of an ordered two-dimensional phase at the electrode−electrolyte interface. The appearance of the capacitance pit while the electrode was at the potential of zero charge (pzc) was supported by measurements first made at the mercury−water interface.[76] ECSTM images were presented of the electrode while in the capacitance pit and showed a periodic structure that was interpreted as the adsorbate lattice structure. These were compared to images of the electrode obtained outside the capacitance pit but were not shown. The ECSTM images of the adsorbate were interpreted in terms of the available crystal structures of adenine chlorides, which implicated the inclusion of chloride ions. Heckl (1993) used STM in air to study adenine on graphite surfaces and by comparison of the adsorbate with the underlying substrate, determined a coincident adsorbate mesh ($a = 1.97$ nm, $b = 1.1$ nm, $\gamma = 90°$ where a was parallel to the substrate vector g and was eight whole substrate lattice constants, $a = 8g$). The STM images were interpreted in terms of a close-packed planar-arranged structure stabilized by intermolecular hydrogen bonds and van der Waals packing constraints. Tao and Shi (1994) used in situ AFM to reexamine adenine monolayer formation on graphite surfaces in 0.1 M NaCl electrolyte. By examining both the adsorbate and substrate structures, the adsorbate coincident lattice was determined ($a = 2.2$ nm $\pm$ 0.5, $b = 0.85 \pm 0.2$ nm, $\gamma = 90 \pm 2°$ where $a = 9\ g$ and $b = 2\sqrt{3}g$). The lateral dimensions agreed well with that determined by Allen et al. (1991) in air. A further STM investigation in air by Sowerby et al. (1996) of adenine films prepared by evaporation of aqueous solutions supported these coincident adsorbate lattice measurements. They presented an image of both the adsorbate and the substrate obtained in a single STM image frame and allowed precise determination of the adsorbate epitaxy. Both Tao and Shi (1994) and Sowerby et al. (1996) proposed different configurations of planar-arranged close-packed hydrogen-bonded models and in agreement with Heckl (1993), excluded both water and ions from the adsorbate structure. The application of complementary techniques to monolayer structure determination led to a further refinement of the adenine adsorbate structure on graphite. Freund et al. (1997) applied LEED to adenine monolayer films grown on graphite by molecular beam epitaxy in ultrahigh vacuum (UHV). They showed symmetry information about the adsorbate that was not obvious in the STM and AFM analyses except following retrospective examination. The LEED analysis confirmed the coincident lattice mesh dimensions previously determined[1,36,37,44] and additionally showed that the adsorbate formed a centered rectangular lattice in a *P*2*gg* plane group. This can clearly be seen in the real space in situ AFM image previously presented.[44] Although the *P*2*gg* plane group was composed of centrosymmetric dimers related by glide symmetry operations, Freund et al. (1997) recognized that adenine could form three possible adenine−adenine dimer

configurations with a 2-fold symmetry axis. MM was used to differentiate between competing structural models on the basis of energy minimization convergence criteria, energy calculations, and preservation of the experimentally observed symmetry conditions. Their final structure could reproduce the LEED reflections in a kinematic LEED simulation; however, the molecules were tilted with respect to the surface. In a reappraisal of the MM simulation, Edelwirth et al. (1997) refined the adsorbate structure. In the minimized configuration, the adenine molecules lay flat on the surface with a maximized van der Waals interaction and realized the maximum number of possible intermolecular hydrogen bonds between adjacent molecules. The adsorbate−substrate interaction was determined to be predominantly of the van der Waals type adequately described by a Lennard-Jones 12-6 potential. The electrostatic component was negligible. The calculated adsorption energy (21 kcal mol^{-1} $Å^{-1}$) compared well with that determined by thermal desorption spectroscopy measurements (23 kcal mol^{-1} $Å^{-1}$). Reiter et al. (1997) presented STM images in air of the adenine adsorbate on graphite surfaces. They have invoked the model of Edelwirth et al. (1997) to interpret the STM contrast of their images.

We have performed MM simulations and energy calculations on the previously proposed packing configurations. Despite complete validity only for the modeling strategy applied to clean surfaces in UHV, we draw the reader's attention to the UHV studies of adenine films on graphite, which have isostructural dimensions, to adenine films prepared on graphite from solution. Although these systems might not be directly comparable, the monolayer structures examined here were all formed through spontaneous self-organization following molecular beam epitaxy in UHV or from aqueous solution with no applied potential to the surface.

Allen et al. (1991,1992) failed to describe the coincident lattice, although it was inherent in their experimentally determined measurements and their proposed lattice model. Following energy minimization, the end configuration (Figure 2A) differs little from the starting configuration (not shown). This is not surprising, since molecular dynamics simulation was employed in their structure determination, although details of the simulation parameters were not shown. The present MM simulation did assign hydrogen-bonding interactions that were not described by Allen et al. (1991, 1992). Both Tao and Shi (1994) and Sowerby et al. (1996) proposed similar structures invoking close-packed hydrogen-bonded monolayers of planar-arranged molecules in a centrosymmetric dimer configuration. Minimization of the structure proposed by Tao and Shi (1994) (Figure 2C) shows marked deviation from the starting configuration (Figure 2B), yet the molecules remain planar and are rearranged to accommodate the maximum number of possible hydrogen bonds. Little change is seen in the structure proposed by Sowerby et al. (1996) following minimization (Figure 2D), and the structure proposed by Edelwirth et al. (1997) was already minimized (Figure 2E).

To compare the models in terms of energetics, we calculated total and component nonbond lattice energies for the minimized models (Table 1). We also calculated the lattice energy for a single molecule within the monolayer structure (ΔE_T). These values indicate that the model proposed by Allen et al. (1991) is energetically less favorable owing to the more positive energy. The structure proposed by Sowerby et al. (1996) gave the best packing with the largest van der Waals interaction. Despite the van der Waals term being the largest contributor to the adsorbate lattice energy, the calculations clearly indicate that the hydrogen bonding and electrostatic components determine the optimal configuration in these polar molecules. It is interesting to note that the energy-minimized structure in Figure

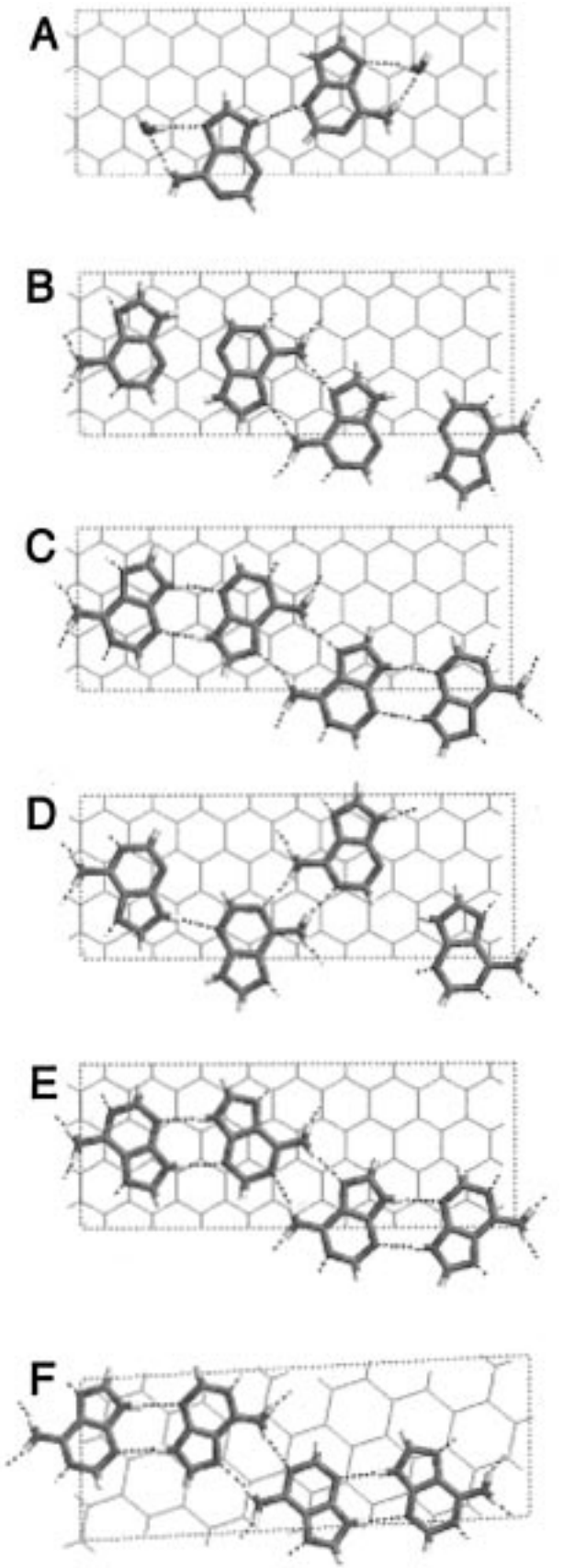

Figure 2. Energy-minimized lattice models of adenine on graphite (A,[36,37] B start configuration,[44] C end configuration, D,[1] E[55]) and MoS_2 (F[32]). The hydrogen bonds are indicated by the dotted lines.

TABLE 1: Energy Calculations Based on MM Simulations of the Published Models of Adenine on Graphite[a]

model	E_T	E_{vdW}	$E_{Coloumbic}$	E_H	ΔE_T
Figure 2A 2 molecules/cell	−75.7	−53.4	−9.0	−13.4	−26.1
Figure 2C 4 molecules/cell	−121.8	−73.7.0	−17.1	−31.0	−35.4
Figure 2E 4 molecules/cell	−121.0	−82.1	−14.1	−24.8	−34.4
Figure 2D 4 molecules/cell	−128.6	−74.6	−19.2	−34.9	−38.0

[a] Energy values given in kcal mol^{-1} $Å^{-1}$.

2C and that proposed by Edelwirth et al. (1997) (Figure 2E) are similar in that they both satisfy the maximum number of possible intermolecular hydrogen bonds. The similarity in the structures is also expressed by their almost identical van der Waals component in the energy calculations (Table 1). Since both models implicate centrosymmetric dimers, the structural difference can be understood in terms of the absence of the glide reflections in the minimized Figure 2C structure. Even though the formation of the centrosymmetric dimers cancels the large dipole moment of the individual molecules, the electrostatic and the hydrogen-bonding components of the dimers to the adsorbate energetics are not fully optimized unless in the *P2gg* configuration as in Figure 2E. The calculations indicate that the model proposed by Edelwirth et al. 1997 is most likely based on energy arguments.

Adenine monolayer formation has also been examined by STM in air on the (0001) surface of MoS_2.[1,32,39] Similarly, variant STM observations resulted in the presentation of different unit mesh dimensions ($a = 1.10$ nm, $b = 0.96$ nm, $\gamma = 85°$;[39] $a = 1.09$ nm, $b = 0.84$ nm, $\gamma = 70 \pm 2°$ [1]). A subsequent and extensive reexamination of the adenine adsorbate on MoS_2 showed the effect of changes in the scan angle of the STM tip on the adsorbate image contrast.[32] Although the apparent contrast showed drastic changes, comparison of the adsorbate images with the underlying substrate showed invariant adsorbate lattice dimensions. This analysis was complicated by the presence of two symmetrically equivalent adsorbate structures, an observation made in an earlier study.[1] MM was also applied to this system and showed that the packing configuration determined by Edelwirth et al. (1997) was most likely. The other structures tested included the previously proposed structures for adenine on graphite and MoS_2 but were energetically unfavored. The energy-minimized model of adenine on MoS_2 (Figure 2F) and the refined lattice dimensions for this system ($a = 2.28$, $b = 0.84$ nm, $\gamma = 93°$) reflect the similarity in the adsorbate lattice structure of adenine on graphite ($a = 2.21$, $b = 0.85$ nm, $\gamma = 90°$) but show the effect of substrate influence on the adsorbate structure. The presence of two symmetrically equivalent adsorbate structures related only by a reflection in the plane perpendicular to the substrate surface supports a possible prebiotic function for enantiomorphic monolayers in localized chiral symmetry breaking.[1]

Furukawa et al. (1997) have used STM in UHV to study adenine films deposited on a Cu(111) surface. They have proposed a model for the adsorbate structure ($a = 2.18$, $b = 0.95$ nm, $\gamma = 90°$) with an almost identical molecular configuration determined for adenine on both graphite and MoS_2 surfaces (parts E and F of Figure 2).[32,55] However, in the absence of substrate data, which were not presented, and with the inherent information concerning adsorbate epitaxy, registration, and calibration, it is difficult to subject their model to a reasonable MM simulation. On the basis of energy-minimization arguments of adenine on graphite and MoS_2 surfaces, it would seem likely that a similar structure would form on other surfaces.

Guanine Monolayers. The structure of guanine monolayers has been addressed by Srinivasan et al. (1991) using ECSTM in a 0.1 MNaCl electrolyte on graphite surfaces. Like adenine,[43] they observed a capacitance pit and presented images of the adsorbate and of the underlying substrate. The periodic features that they presented were interpreted in terms of the lattice structure of the guanine monohydrate crystal (301) plane, which positions the molecules in the *P2gg* plane group configuration.

Tao and Shi (1994) reexamined the guanine monolayer structure in 0.1 M NaCl electrolyte on graphite surfaces using both ECSTM and in situ AFM techniques. They reported two possible adsorbate structures. The first coincident mesh, type I, described a superperiodic feature observed in the STM images ($a = 0.85 \pm 0.2$ nm, $3b = 3.30 \pm 1.5$ nm, $\gamma = 90 \pm 2°$, where $a = 2\sqrt{3}g$ and $3b = 14g$ [44]). The occurrence of a second different structure, type II, was inferred by an image obtained at an adsorbate domain boundary. For this adsorbate structure they described an oblique coincident mesh (the lattice vectors were reassigned for easy comparison $2a = 1.92$ nm, $b = 0.98$ nm, $\gamma = 97.3°$, where $b = 4g$). In both models, Tao and Shi (1994) proposed a planar arrangement of molecules stabilized by intermolecular hydrogen bonds. There are, however, severe difficulties with their assignment of these interactions in their type I structure, with hydrogen bonds, in some cases where there are no proton donors.[44] The proposed type II packing structure[45] seemed more realistic with the formation of centrosymmetric dimers through conventional hydrogen bond interactions.

Following MM simulations, the type I structure of Tao and Shi (1994) failed to reach a minimized structure even after 500 minimization cycles (not shown) and the molecules tended to stand with their planar rings perpendicular to the surface, apparently driven by their propensity to stack.[73] In the final minimized structure of the proposed type II configuration[45] (Figure 3A), the molecules remained reasonably planar, although a tilt of 7° between the planar rings and the graphite surface was measured and suggests that the unit mesh dimensions are too restricting to accommodate a planar arrangement of four guanine molecules. This configuration also resulted in the assignment of three-center hydrogen bonds, which have not been described previously for guanine−guanine interactions.

Poler et al. (1995) used thermopower STM to investigate guanine monolayers prepared by evaporation of aqueous solutions on graphite surfaces. They described a monolayer structure implicating water molecules hydrogen-bonded to guanine molecules. They incorrectly invoked similar models previously proposed by Heckl et al. (1991) of a comparable system that explicitly described close-packed adsorbate models of guanine monolayers on graphite without included water.[38] In the absence of the coincident mesh data it is difficult to subject their model to scrutiny by MM.

STM in air allowed Heckl et al. (1991, 1993) to examine guanine monolayers prepared by evaporation of aqueous solutions on both graphite and MoS_2 surfaces. By presentation of images of both the adsorbates and their underlying substrates, coincident unit meshes for the adsorbates could be described in terms of their underlying substrate lattices. On graphite, the adsorbate formed a rectangular mesh ($2a = 2.13$ nm, $b = 1.97$ nm, $\gamma = 90°$, where $b = 8g$). The observed lattice dimensions were not congruent with either of those described above.[44,45] On MoS_2 an oblique guanine mesh was formed ($2a = 2.21$ nm, $b = 1.92$ nm, $\gamma = 95 \pm 2°$, where $2a = 7g$). There was no

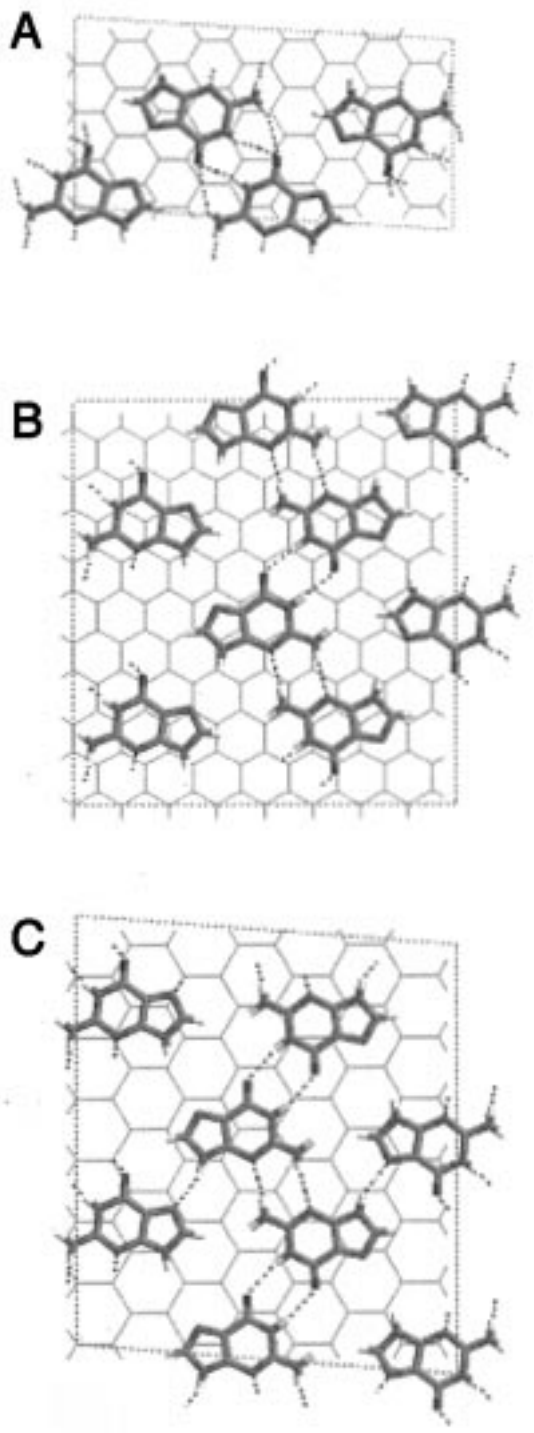

Figure 3. Energy-minimized lattice models of guanine on graphite (A,[45] B[38,39]) and MoS_2 (C[38,39]).

discussion concerning the presence or absence of symmetrically equivalent structures.[38,39] The models presented had packing configurations identical with a planar arrangement of symmetrically hydrogen-bonded dimers. The application of MM to these systems yielded convincing arguments for the plausibility of the proposed structures. In the energy-minimized models (parts C and D of Figure 3), the molecules are lying flat on the substrate surfaces with the maximized van der Waals interaction. These configurations mimic the adenine structure with the preservation of the *P*2*gg* molecular configuration, and the tendency to form a rectangular mesh on graphite and an oblique mesh on MoS_2; however, not all possible hydrogen bonds were realized. Determination of the molecular lattice energy for guanine on graphite (Table 2) shows a value per molecule lower than that calculated for the structure proposed by Tao and Shi (1994).

TABLE 2: Energy Calculations Based on MM Simulations of the Published Models of Guanine on Graphite[a]

model	E_T	E_{vdW}	$E_{Coloumbic}$	E_H	ΔE_T
Figure 3A 2 × 4 molecules/cell	−262.0	−162.3	−42.9	−56.8	−37.2
Figure 3B 8 molecules/cell	−308.7	−189.8	−75.5	−43.5	−47.7
Figure 4C 2 × 4 molecules/cell	−305.2	−173.7	−77.7	−53.7	−48.0

[a] Energy values given in kCal/mol/Å.

We have examined further STM data of guanine prepared on graphite by evaporation of aqueous solution and have found no evidence to suggest any polymorphic variants. There is some consistency between the observed coincident lattice dimensions from the Tao and Shi model type II ($2a = 1.92$ nm, $b = 0.98$ nm, $\gamma = 97.3°$, where $b = 4g$) and that of Heckl et al. (1991, 1993) ($2a = 2.13$ nm, $b = 1.97$ nm, $\gamma = 90°$, where $b = 8g$) where the linear dimensions of *b* are related by a simple factor of 2. This is because Heckl et al. (1991, 1993) describes an adsorbate lattice that is coincident with the substrate at every second adsorbate lattice position in the *b* direction, whereas Tao and Shi (1994) assume that every equivalent position is coincident with the underlying substrate. We have been unable to reassess some of the previously published data, since the substrate STM images were not included in the publication.[45] Our own images of the guanine adsorbate obtained in the same frame as the underlying graphite substrate allow for an internal calibration of the adsorbate data (parts A and B of Figure 4) and provide convincing arguments for a different interpretation that is incongruent with any of the data previously presented. The coincident adsorbate lattice dimensions ($a = 1.07$ nm, $b = 1.86$ nm, $\gamma = 90°$) are almost identical with that determined by Heckl et al. (1991, 1993), the difference being the orientation of the mesh with respect to the substrate and that every equivalent adsorbate contrast is coincident with the underlying substrate. Both Heckl et al. (1991, 1993) and Tao and Shi (1994) described a coincident lattice vector *b* parallel to the substrate vector *g*. However, images at natural monolayer island edges (Figure 4A) and images obtained by deliberately rupturing the adsorbate structure (Figure 4B) show that the underlying substrate *g* lattice direction is not quite parallel to the adsorbate *b* direction. The coincident adsorbate lattice vector *b* is described by $b = 7g_1 + 1g_2$. Reexamination of the experimental data of Heckl et al. (1991, 1993) showed that 5 min had elapsed between acquisition of the adsorbate and substrate images and provides an explanation of the deviation in terms of the thermal drift of the STM instrument. Energy minimization of guanine molecules in a *P*2*gg* configuration on the proposed coincident lattice resulted in a planar-arranged adsorbate structure that satisfied the maximum number of conventional intermolecular hydrogen bonds (Figure 4C) and in that sense reproduces the structural configuration for adenine monolayers. The energy determined per molecule also favored this structure as being the most stable albeit by a small value (0.3 kcal mol^{-1} $Å^{-1}$). On the basis of the energy calculation arguments, the *P*2*gg* structure (Figure 4C) would be the most stable.

Summary

The analyses of the adenine and guanine adsorbates on both graphite and MoS_2 surfaces demonstrate the problems inherent

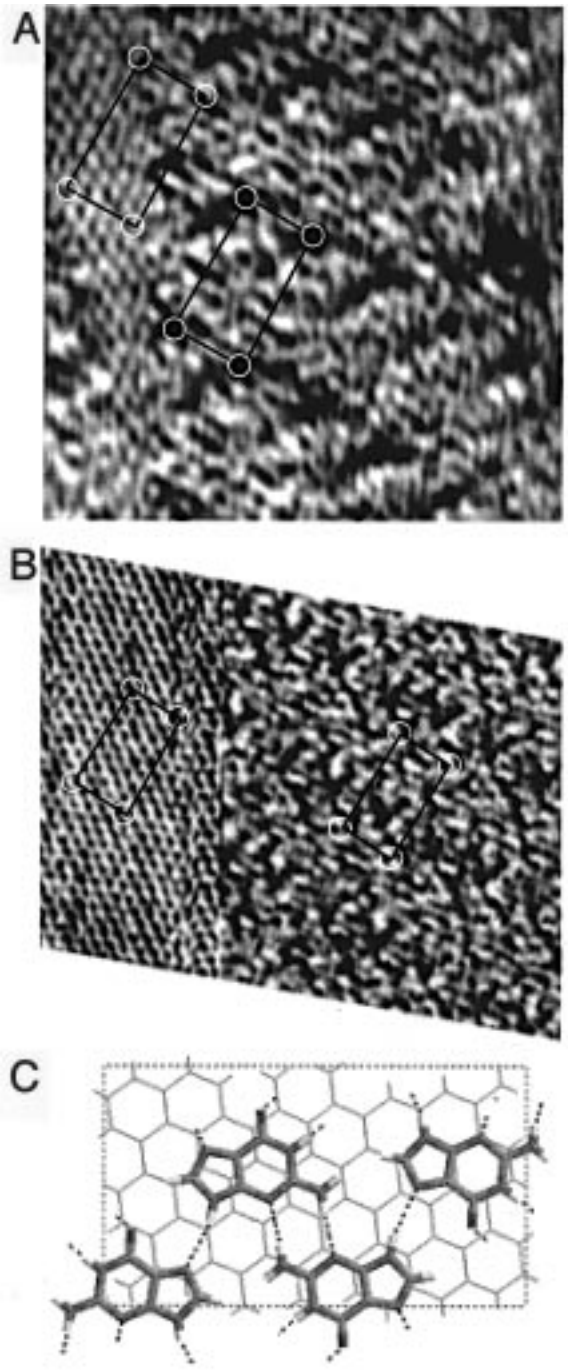

Figure 4. (A) STM image of a natural guanine monolayer island edge on the surface of graphite. Further details of the STM imaging parameters and instrumentation can be found in Heckl et al. (1991). (B) STM image showing an ordered array of guanine molecules adsorbed onto the HOPG surface (imaging parameters: bias voltage = 800 mV; tunnel current = 200 pA) and, in the same frame, the underlying substrate showing the uppermost carbon atoms of HOPG, 0.246 nm apart, obtained by reducing the bias voltage so that the STM tip pierced the adsorbate to image the substrate (imaging parameters: bias voltage = 20 mV; tunnel current = 200 pA). The image frame shows both adsorbate and substrate data simultaneously and allows the position of the adsorbate molecules on the substrate to be determined precisely. Further details of the STM imaging parameters and instrumentation can be found in Sowerby et al. (1996). Both images reveal the underlying graphite substrate atoms 0.246 nm apart and provide an internal calibration for the adsorbate image. The images have been geometrically corrected on the basis of the adsorbate component and show the adsorbate lattice that is coincident with the underlying substrate (C). The energy-minimized lattice model of guanine on graphite is based on the dimensions determined in A and B.

in the direct interpretation of STM and AFM image data. Although it is conceivable that different packing configurations may be present as polymorphs, examination by surface averaging LEED rules out this possibility for the vacuum-deposited adenine monolayers.[54] It is unlikely that there are different polymorphic structures for the adenine monolayer on graphite because of the consistency of the experimentally determined lattice dimensions. Determination of the energy differences between polymorphic (α,β,γ)-glycine crystals by the atom−atom potential method shows values of approximately 1 kcal mol^{-1} $Å^{-1}$,[67] substantially less than that determined here for the adenine monolayer structures. This suggests inaccuracies in the interpretation of the STM data and the application of model building. Heckl (1993) revised his interpretation of the adenine adsorbate mesh dimensions after reexamination of the STM images.[54] The anisotropic response of the STM images of adenine on MoS_2 to changing scan angle is probably due to a complicated mixture of the organic heterocycle and the cyclic hydrogen bond components of the structure.[32] The effective smearing of the lattice features in these STM images may have contributed to the earlier inaccuracies in the determination of the precise adsorbate coincident mesh.[1,39]

Similarly, it seems unlikely that guanine forms polymorphs, although arguments for the formation of different packing structures that include either ions or water might be supported by the Tao and Shi (1994) types I and II coincident lattices observed in electrolytes. We have never observed these in evaporated guanine samples.

The primary source of error in structure determination using STM and AFM images of molecular adsorbates can occur during the acquisition of the raw image data. This is primarily concerned with the calibration of the STM/AFM images of the molecular adsorbates, which have initially unknown configurations and periodic dimensions. Typically, adsorbate images are calibrated against images of the underlying substrate, which have a well-defined geometry and lateral dimensions. Images of both the adsorbate and the underlying substrate can be obtained in the same image frame. This allows for an internal standard calibration for the adsorbate lattice features but can also be informative in the determination of the precise adsorbate epitaxy.[1,55,56] These images can be obtained at naturally occurring monolayer island edges or can be induced by deliberately rupturing the adsorbate partway through the image scan. In the absence of these data, it has been our experience that images of the *directly* underlying substrate should be obtained as quickly as possible, since even over very short periods of time, small variations in the scanning parameters or physical location on the surface can occur as a result of thermal drift, which has significant consequences at atomic scale dimensions. Images of the substrate obtained at different locations run the risk of being on different substrate domains and consequently rotated with respect to the adsorbate. Although this is less likely on single-crystal electrodes, it is common on graphite surfaces. Obtaining images of the adsorbate and the substrate at different scan sizes should be avoided unless it can be verified that the piezoelectric scanning mechanism scales linearly over the atomic dimensions being examined. We would argue that adsorbate images are only of limited value unless accompanied by images of the *directly* underlying substrate acquired at the same scan size and within a few minutes of the adsorbate image. The use of both MoS_2 and graphite substrates allows comparison of the molecular contrast by STM because of differences in coupling of the adsorbate molecular states.[38] This results in STM images of

the adsorbates as whole molecular structures on MoS_2 and in some cases indicates the positions of intermolecular hydrogen bonds,[32,41,56] whereas on graphite, the detail is consistent with submolecular detail.

Following the precise determination of the adsorbate coincident dimensions, assessment of the adsorbate packing configuration is best achieved by employing complementary structure-resolving techniques such as LEED; however, in the absence of such data, the application of MM simulation to differentiate between packing structures and coincident structures seems to give sensible results. The available literature on the molecular packing of the bulk state may also be informative. Examining STM/AFM data obtained at adsorbate domain boundaries can show the effect of the scanning direction on the image contrast. This effect has previously been explored in a study that investigated the effect of scan angle on STM image contrast.[32] In the absence of a detailed characterization of the STM image contrast as a function of scan angle, it could be easy to misinterpret different contrasts of the same structure as different packing configurations.

In the energy-minimized models of the adenine and guanine adsorbates on graphite and MoS_2 surfaces, the consistent feature is the *P*2*gg* plane group motif, which is also seen for uracil monolayers on these surfaces and which is similarly minimized following MM simulation.[56] On graphite these structures form a centered rectangular lattice in the *P*2*gg* plane group; however, on MoS_2 the structure is skewed in to an oblique lattice of *P*2 symmetry but maintaining the approximate molecular arrangement. This is probably due to a higher adsorbate−substrate interaction on MoS_2 than on graphite surfaces.[57] On graphite the uracil monolayer is almost identical with that of its bulk state;[41,56] however, the bulk state configurations of adenine and guanine have not been available, so a simple comparison is not possible. Central to the adsorbate structures are the formation of the centrosymmetric dimers, which neutralize the strong dipole moments of the individual molecules. π-Bond cooperativity, which contributes to the stability of cyclic hydrogen bonds between complementary base pairs in nucleic acids, requires that adjacent hydrogen-bonding functional groups are linked by bonds with π-electron character.[75] These structural motifs are also reproduced in the monolayer configurations of the pure bases. The centrosymmetric dimers are linked to two adjacent dimers through nonsymmetrical cyclic or single hydrogen bonds in a *P*2*gg* molecular configuration, which also appears to be electrostatically optimized. If these energy-minimizing principles are consistent, then the structures should remain essentially invariant in their configuration when physisorbed at the solid−liquid interface, although their precise positions could be modified slightly by the adsorbate−substrate interaction. These minor variations may have had consequences at the prebiotic solid−liquid interface.

Acknowledgment. S. J. Sowerby thanks the Alexander von Humboldt-Stiftung for a postdoctoral research fellowship. Support is from Deutsche Forschungsgemeinschaft through He 1617/3-1/3-2/6-1.

References and Notes

(1) Sowerby, S. J.; Heckl, W. M.; Petersen, G. B. *J. Mol. Evol.* **1996**, *43*, 419.
(2) Sowerby, S. J.; Heckl, W. M. *Origins Life Evol. Biosphere* **1998**, *3*, 1.
(3) Ferris, J. P.; Hagen, J. W. J. *Tetrahedron* **1984**, *40* (7), 1093.
(4) Shapiro, R. *Origins Life Evol. Biosphere* **1995**, *25*, 83.
(5) Bernal, J. D. *The Physical Basis of Life*; Routlege and Keegan Paul: London, 1951.
(6) Cairns-Smith, A. G. *Genetic takeover and the mineral origins of life*; Cambridge Univiversty Press: Cambridge, 1982.
(7) Russell, M. J.; Hall, A. J.; Cairns-Smith, A. G.; Braterman, P. S. *Nature* **1988**, *336*, 117.
(8) Russell, M. J.; Hall, A. J.; Turner, D. *Terra Nova* **1989**, *1*, 238.
(9) Wächtershäuser, G. *Microbiol. Rev.* **1988**, *52*, 452.
(10) Binnig, G.; Rohrer, H.; Gerber, C.; Weibel, E. *Phys. Rev. Lett.* **1982**, *49* (1), 57.
(11) Binnig, G.; Quate, G. C.; Gerber, C. *Phys. Rev. Lett.* **1986**, *56*, 930.
(12) Park, S.; Quate, G. C. *Appl. Phys. Lett.* **1986**, *48*, 112.
(13) Weimer, M.; Kramar, C. B.; Baldeschwieler, J. D. *Phys. Rev. B* **1988**, *37* (8), 4292.
(14) Stupian, G. W.; Leung, M S. *Appl. Phys. Lett.* **1987**, *51* (19), 1560.
(15) Eggleston, C. M.; Hochella, M. F., Jr. *Geochim. Cosmochim. Acta* **1990**, *54*, 1511.
(16) Eggleston, C. M.; Hochella, M. F., Jr. *Am. Mineral.* **1992**, *77*, 221.
(17) Fan, F. R.; Bard, A. J. *J. Chem. Phys.* **1991**, *95*, 1969.
(18) Colell, H.; Bronold, M.; Fiechter, S.; Tritbusch, H. *Surf. Sci. Lett.* **1994**, *303*, L361.
(19) Eggleston, C. M.; Hochella, M. F., Jr. *Science* **1991**, *254*, 983.
(20) Sharp, T. G.; Zheng, N. J.; Tsong, I. S. T.; Buseck, P. R. *Am. Mineral.* **1990**, *75*, 1438.
(21) Eggleston, C. M.; Hochella, M. F., Jr. *Am. Mineral.* **1993**, *78*, 877.
(22) Higgins, S. R.; Hammers, R. J. *Geochim. Cosmochim. Acta* **1996**, *60*, 3067.
(23) Cotterill, G. F.; Bartlett, R.; Hughes, A. E.; Sexton, B. A. *Surf. Sci. Lett.* **1990**, *232*, L211.
(24) Higgins, S. R.; Hammers, R. J. *Surf. Sci.* **1995**, *324*, 263.
(25) de Levie, R. *Chem. Rev.* **1988**, *88*, 599.
(26) Heckl, W. M.; Engel, A. Imaging nucleic acids with scanning probe microscopes. In *Visualization of Nucleic Acids*; Morel, G., Ed.; CRC Press: Boca Raton, FL, 1995; p 21.
(27) Wirth, M. J.; Fatnumbi, H. O. *LC−GC* **1994**, *12* (3), 222.
(28) Swalen, J. D.; et al. *Langmuir* **1987**, *3* (932), 932.
(29) Parkins, R. N. *Comprehensive Treatise of Electrochemistry*; Bockris, J. O. M., et al., Eds.; Plenum Press: New York, 1980; Vol. 4.
(30) Russell, V. A.; Ward, M. D. *Chem. Mater.* **1996**, *8*, 1654.
(31) Heckl, W. M.; Holzrichter, J. F. *Mol. Cryst. Liq. Cryst. Sci. Technol. B* **1992**, *2*, 231.
(32) Sowerby, S. J.; Edelwirth, M.; Reiter, M.; Heckl, W. M. *Langmuir*, in press.
(33) Ludwig, C.; Gompf, B.; Petersen, J.; Strohmeier, R.; Eisenmenger, W. *Z. Phys.* **1994**, *B93*, 365.
(34) Cyr, D. M.; Venkataraman, B.; Flynn, G. B. *Chem. Mater.* **1996**, *8*, 1600.
(35) Smith, D. P. E.; Heckl, W. M.; Klagges, H. A. *Surf. Sci.* **1992**, *278*, 166.
(36) Allen, M. J.; Balooch, M.; Subbiah, S.; Tench, R. J.; Siekhaus, W.; Balhorn, R. *Scanning Microsc.* **1991**, *5* (3), 625.
(37) Allen, M. J.; Balooch, M.; Subbiah, S.; Tench, R. J.; Balhorn, R.; Siekhaus, W. *Ultramicroscopy* **1992**, *42−44*, 1049.
(38) Heckl, W. M.; Smith, D. P. E.; Binnig, G.; Klagges, H.; Hänsch, T. W.; Maddocks, J. *Proc. Natl. Acad. Sci. U.S.A.* **1991**, *88*, 8003.
(39) Heckl, W. M. *Rastertunnelmikroskopie an zweidimensionalen Kristallen aus organischen Molecülen*; Ludwig Maximilians Universität München, Habilitationsschrift: Germany, 1993.
(40) Reiter, M.; Edelwirth, M.; Heckl, W. M.; Sowerby, S. J. *Probe Microsc.*, in press.
(41) Sowerby, S. J.; Petersen, G. B. *J. Electroanal. Chem.* **1997**, *433*, 85.
(42) Srinivasan, R.; Murphy, J. C.; Fainchtein, R.; Pattibiraman, N. *J. Electroanal. Chem.* **1991**, *312*, 293.
(43) Srinivasan, R.; Murphy, J. C. *Ultramicroscopy* **1992**, *42−44*, 453.
(44) Tao, N. J.; Shi, Z. *J. Phys. Chem.* **1994**, *98*, 1464.
(45) Tao, N. J.; Shi, Z. *J. Phys. Chem.* **1994**, *98*, 7422.
(46) Tao, N. J.; Shi, Z. *Surf. Sci. Lett.* **1994**, *321*, L149.
(47) Tao, N. J.; Shi, Z. *Surf. Sci. Lett.* **1994**, *301*, L217.
(48) Poler, J. C.; Zimmerman, R. M.; Cox, E. C. *Langmuir* **1995**, *11*, 2689.
(49) Dretschkow, T.; Dakkouri, A. S.; Wandlowski, T. *Langmuir* **1997**, *13*, 2843.
(50) Tao, N. J.; DeRose, J. A.; Lindsay, S. M. *J. Phys. Chem.* **1993**, *97*, 910.
(51) Nakagawa, T.; Tanaka, H.; Kawai, T. *Surf. Sci. Lett.* **1997**, *370*, L1444.
(52) Kawai, T.; Tanaka, H.; Nakagawa, T. *Surf. Sci.* **1997**, *386*, 124.
(53) Furukawa, M.; Tanaka, H.; Kawai, T. Unpublished results.
(54) Freund, J.; Edelwirth, M.; Kröbel, P.; Heckl, W. M. *Phys. Rev. B* **1997**, *55*, 5394.
(55) Edelwirth, M.; Freund, J.; Sowerby, S. J.; Heckl, W. M. *Surf. Sci.*, in press.

(56) Sowerby, S. J.; Edelwirth, M.; Heckl, W. M. *Appl. Phys.* **1998**, *A66*, S549.
(57) Fisher, A. J.; Blöchl, P. E. *Phys. Rev. Lett.* **1993**, *70*, 3263.
(58) Ou-Yang, H.; Marcus, R. A.; Källerbring, B. *J. Phys. Chem.* **1994**, *100*, 7814.
(59) Wang, X. W.; Tao, N. J.; Cunha, F. *J. Phys. Chem.* **1996**, *105*, 3747.
(60) Sautet, P. *Chem. Rev.* **1997**, *97*, 1097.
(61) Mayo, S. L.; Olafson, B. D.; Goddard, W. A., III. *J. Phys. Chem.* **1990**, *94*, 8897.
(62) Weiss, K.; Phillips, J. M. *Phys. Rev. B* **1976**, *14* (12), 5392.
(63) Bondi, C.; Baglioni, P.; Taddei, G. *Chem. Phys.* **1985**, *96*, 277.
(64) Seidel, C.; Awater, C.; Liu, X. D.; Ellerbrake, R.; Fuchs, H. *Surf. Sci.* **1997**, *371*, 123.
(65) Edelwirth, M.; Heckl, W. M.; Sowerby, S. J. Manuscript in preparation.
(66) Steward, E. L.l Foley, C. K.; Allinger, N. L.; Brown, J. P. *J. Am. Chem. Soc.* **1994**, *116*, 7282.
(67) Pertsin, A. J.; Kitaigorodsky. *The atom−atom potential method: Applications to organic molecular solids*; Goldanskii, V. I., Schäfer, P. F., Toennies, J. P., Eds.; Springer-Verlag: Berlin, 1987.
(68) Broomhead, J. M. *Acta Crystallogr.* **1951**, *4*, 92.
(69) Broomhead, J. M. *Acta Crystallogr.* **1948**, *1*, 324.
(70) Cochrane, W. *Acta Crystallogr.* **1951**, *4*, 81.
(71) Kistenmacher, T. J.; Shigematsu, T. *Acta Crystallogr.* **1974**, *B30*, 166.
(72) Kistenmacher, T. J.; Shigematsu, T. *Acta Crystallogr.* **1974**, *B30*, 1528.
(73) Saenger, W. *Principles of nucleic acid structure*; Cantor, C. R., Ed.; Springer Advanced Texts in Chemistry. 1. Nucleic Acids; Springer-Verlag: New York, 1984.
(74) Thewalt, U.; Bugg, C. E.; Marsh, R. E. *Acta Crystallogr.* **1971**, *B27*, 2358.
(75) Jeffrey, G. A.; Saenger, W. *Hydrogen bonding in biological structures*; Springer-Verlag: Berlin, 1994.
(76) Vetterl, V. *Collect. Czech. Chem. Commun.* **1966**, *31*, 2105.